Supplementary information

Experimental Methods

Preparation of perovskite solar cells

All reagents including material were used without further purification. ITO (Indium Tin Oxide) Coated Glass (Liaoning Yike Precision New Energy Technology Co.,Ltd.) and flexible substrates PET/IMI (purchased from OPVIUS GmbH) were ultrasonically cleaned sequentially for 10 minutes in acetone and isopropanol. Then, the substrates were treated under UV-Ozone box for 10 minutes (flexible substrates for 5mins) to remove organic residues and to enable better wetting. For the standard device an aqueous SnO_2 nanoparticle solution (Alfa Aesar) was used to prepare the electron transport layer (ETL). The SnO_2 solution was diluted to 5.0 wt.% and treated in the ultrasonic bath for 10 minutes followed by filtering using a 0.45 µm PTFE filter. The solution was then doctor bladed at 70 °C with 15 mm/s and a gap height of 100 µm. Next, the film was annealed at 150 °C for 30 minutes to form a compact layer. Tin oxide on a flexible PET substrate was annealed at 130 °C for 30 minutes. 2 mg/ml monoFAPA and bisFAPA were dissolved in 1-butanol then blade-coated on top of SnO_2 at 3 mm/s and a gap height of 250 µm and following annealed at 120 °C for 5 min and then washed by isopropanol. Equal molar ratio of MAI (Sigma, 98 %) and PbI_2 (TCI, 99.99%) were dissolved in Dimethylformamide (DMF, Aldrich, 99.8%) with1-methyl-2-pyrrolidinone (NMP, Aldrich, 99.8%), (DMF: NMP, 9:1) to prepare 1.25 M $MAPbI_3$ precursor solution and ultrasonication at room temperature for 10 mins. A mixture was prepared using 1.25 M FAPbI3 along with an additional 10% CsCl, and this mixture was combined with $MAPbI_3$ in a 7:3 ratio. The precursor solution was doctor bladed onto the substrate at 5 mm/s and a gap height of 150 µm. The substrate with the still wet film was treated by air blowing for 10 seconds to get a yellowish perovskite intermediate film followed an annealing process at 150 °C for 10 minutes to get the final perovskite film. The perovskite layer on the flexible substrate was subjected to annealing at 120°C for a duration of 10 minutes. PEDOT (poly(3,4-ethylenedioxythiophene)) (HTL solar 3, purchased from Ossila) is being used as the hole transport layer. A gap height of 250 µm and a volume of 30 µl was used for doctor blading. The blade-coating temperature and speeds for HTL were 60 °C with 10 mm/s, following with annealed at 120°C for 5 minutes. Finally, the carbon paste (Liaoning Yike Precision New Energy Technology Co.,Ltd.) was printed on top of HTL following by annealing on a hot plate at 120°C for 10 minutes.

Preparation of flexible perovskite solar modules

The preparation of flexible perovskite solar modules begins with the patterning of a flexible PET/IMI foil using a femtosecond laser to create P1 lines prior to coating with SnO_2. Subsequently, the patterned conductive flexible foils undergo cleaning via a CO_2 laser. The cleaned flexible foil was prewetted by Florence based-surfactant (Capstone) before coating SnO_2. The layer of SnO_2 (3wt%) is then applied onto the clean, patterned PET/IMI using a roll-to-roll slot die at a flow rate of 0.3 ml/min. The resulting SnO_2 film undergoes transfer to an oven for annealing at 130ºC for a few minutes. Next, the printed SnO_2 substrates are

cut into small pieces for the subsequent printing of the FAPA layer, perovskite, and HTL via doctor blading within a dry air glove box. The stack consisting of PET/IMI/SnO_2/FAPAs/Pero/HTL is then subjected to patterning of P2 lines using a femtosecond laser power of 850mW. Finally, carbon electrodes are printed onto the substrate using a stencil mask to create P3 lines, followed by transfer to a hotplate for annealing for 10 minutes at 120ºC.

Material characterization

XPS measurements were performed (Quantera II, Physical Electronics, Chanhassen, MN, USA) applying a monochromatic Al Kα X-ray source (1486.6 eV) operating at 15 kV and 25 W. The binding energy scale was referenced to the C 1*s* signal at 285.0 eV.

UPS measurements using synchrotron radiation were carried out at the optic beamline at Tübingen Universtiy.

trPL spectra measured carried out with a Fluotime 300 system. The samples were excited by the PDL 820 picosecond diode laser with a wavelength of 402 nm at an average incident power of 4 μW at a frequency of 20000 kHz.

Differential PL lifetime: a differential lifetime constant (π_{PL}) was introduced to quantify the surface recombination from the transient PL of the layered perovskite with the charge transport layer. A differential lifetime as defined by equation with $\pi_{PL}(t) = -\left(\frac{dln(\emptyset_{PL}(t))}{dt}\right)^{-1}$, the advantage of using differential lifetime is that all the decay lifetime involved including charge transfer and interfacial recombination by showing two distinct lifetime constants.

WF measurements were conducted with a Kelvin probe system SKP5050. The contact potential difference between the tip and the samples was measured. The WF of tip can be confirmed by a gold calibration sample.

PLQY was calculated from an absolute PL measurement with integrating sphere. The films are excited with a 405 nm wavelength laser diode. The intensity of laser was calibrated with a power meter and was adjusted to 80 mW cm^{-2}, which is same to the photon flux under AM 1.5G spectra.

EQE spectra were obtained using an EQE measurement system assembled by Enli Technology (Taiwan).

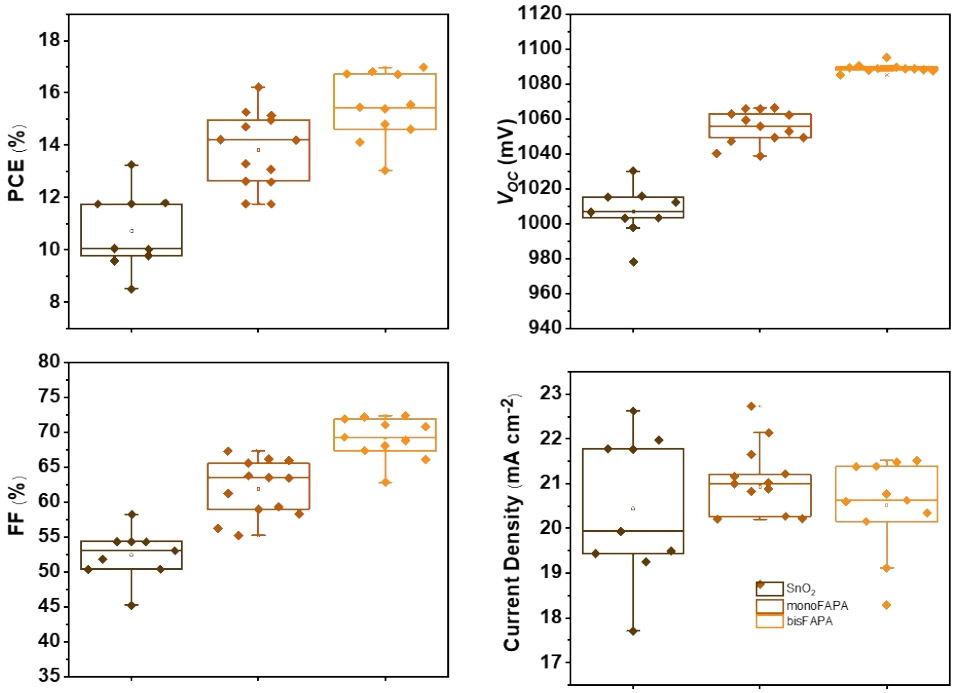

Figure S1. Device performance evaluation of rigid solar cells on SnO_2, monoFAPA and bisFAPA modified SnO_2.

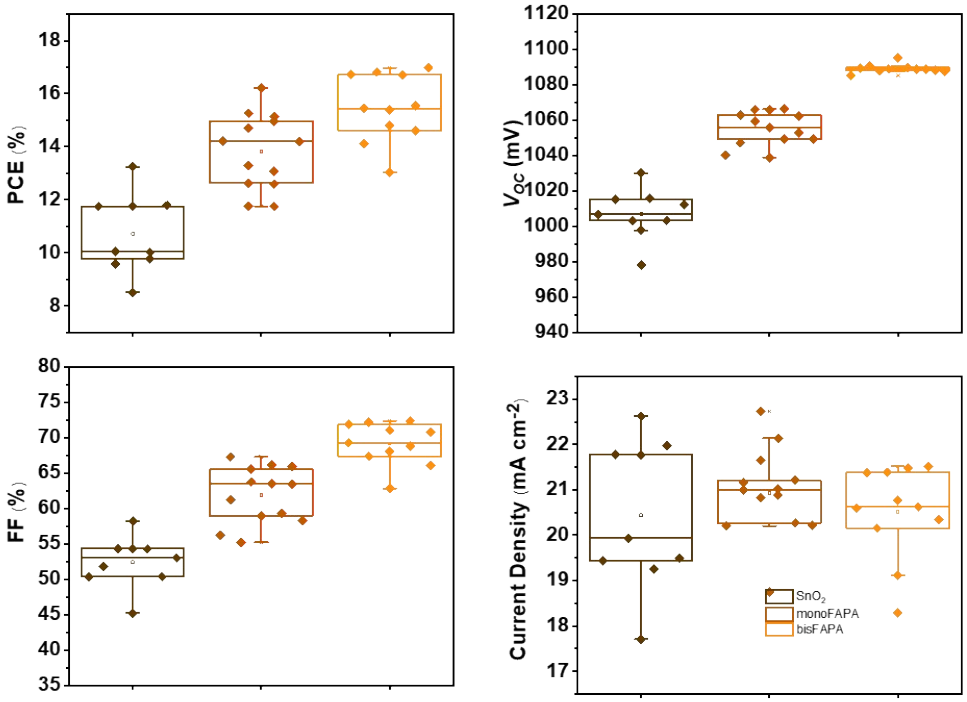

Figure S2. Device performance evaluation of flexible solar cells on SnO_2, monoFAPA and bisFAPA modified SnO_2.

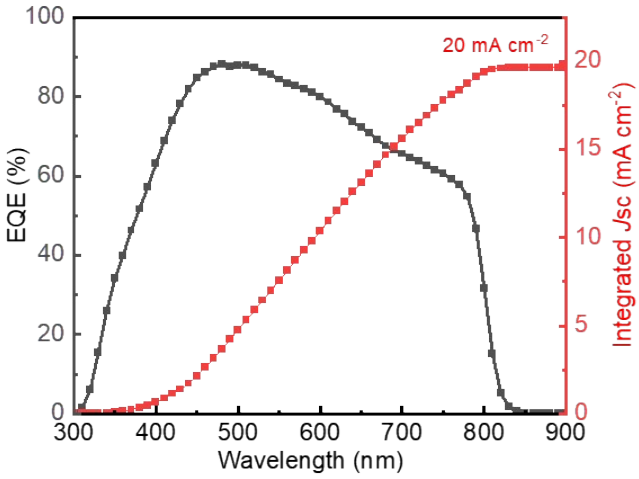

Figure S3. EQE spectrum for the champion cell based on the device structure of PET/IMI/SnO_2/bisFAPA/Perovskite/HTL/Carbon.

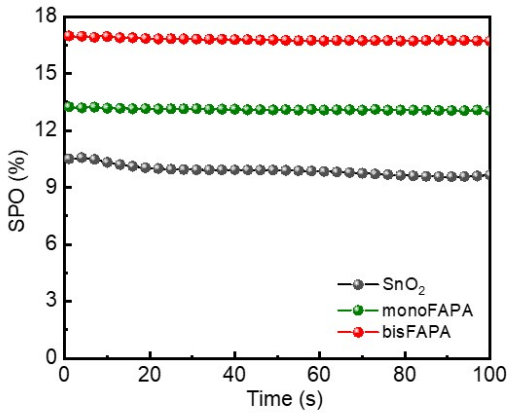

Figure S4. Stabilized output power (SPO) based on SnO_2, monoFAPA and bisFAPA modified flexible devices.

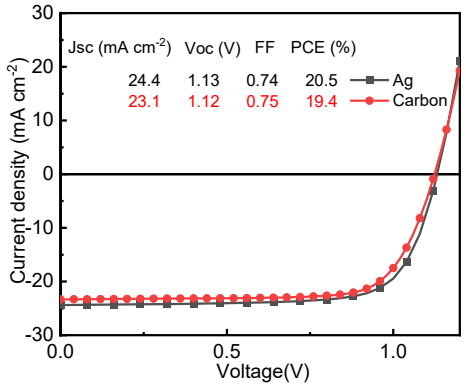

Figure S5. PSCs based on metal electrode and carbon electrode.

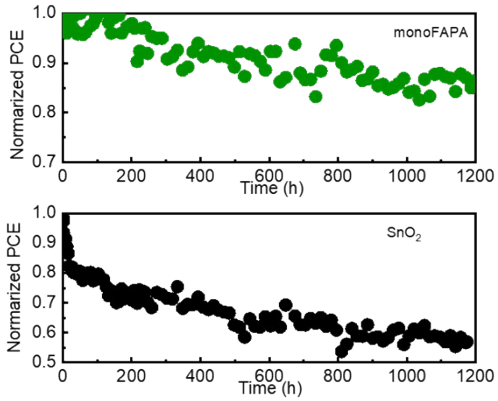

Figure S6. Operational stability of the reference and monoFAPA modified SnO_2 under 1 sun and 65ºC in N_2 atmosphere.

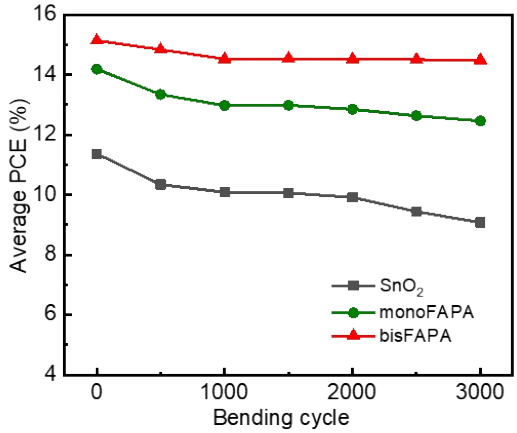

Figure S7. Original average PCE variation based on typical three conditions with a function of bending cycles.

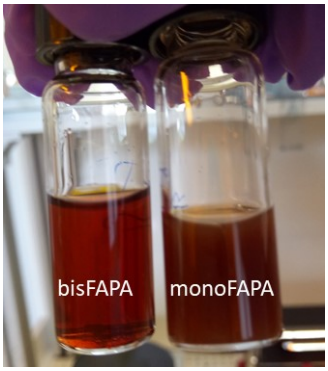

Figure S8. Two FAPAs dissolved in 1-butanol.

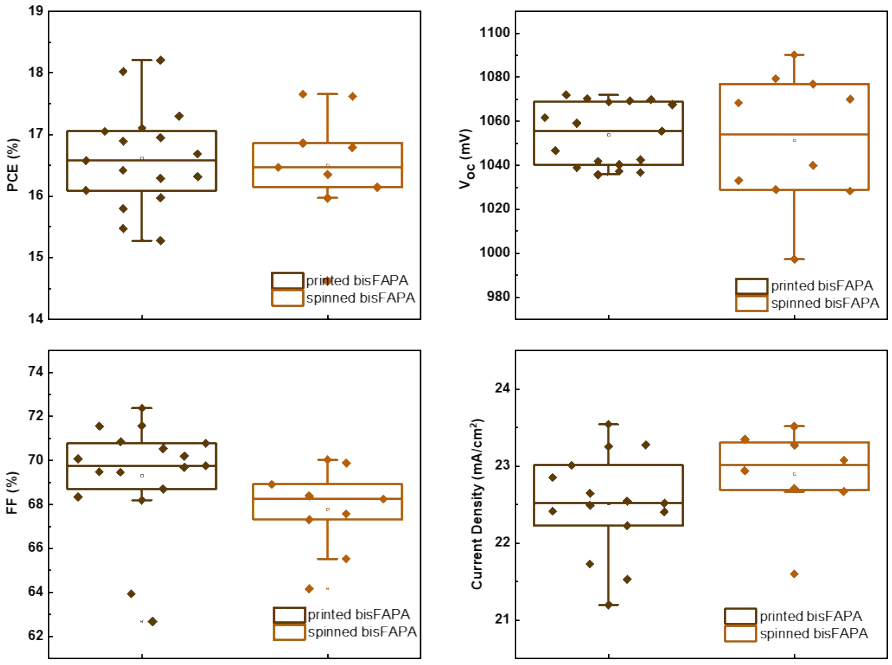

Figure S9. Comparison of device performance on FAPA layers processed using scalable doctor blading and spin-coating methods.

Figure S10. Water contact angle on SnO_2, monoFAPA and bisFAPA modified SnO_2.

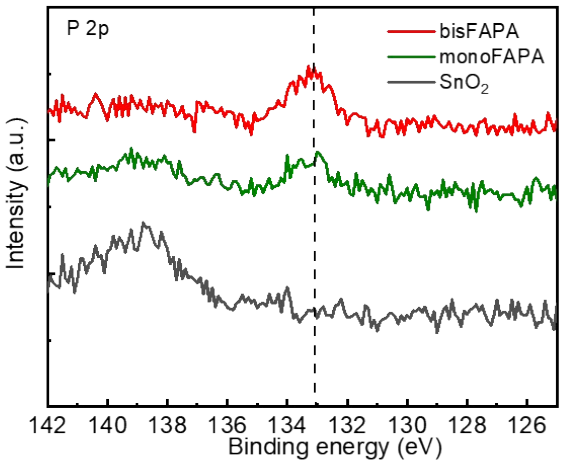

Figure S11. XPS measurement signal illustrating the presence of phosphor element from monFAPA and bisFAPA modified SnO_2 surface.

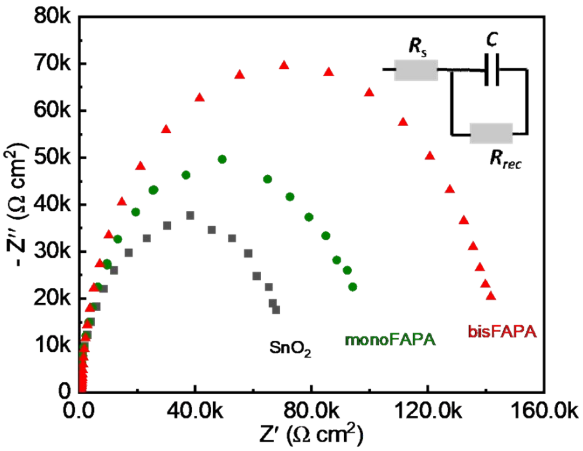

Figure S12. Nyquist plots of perovskite solar cells prepared on bare SnO_2 and SnO_2 interfaces with FAPA modification. The inset shows the corresponding equivalent circuit.

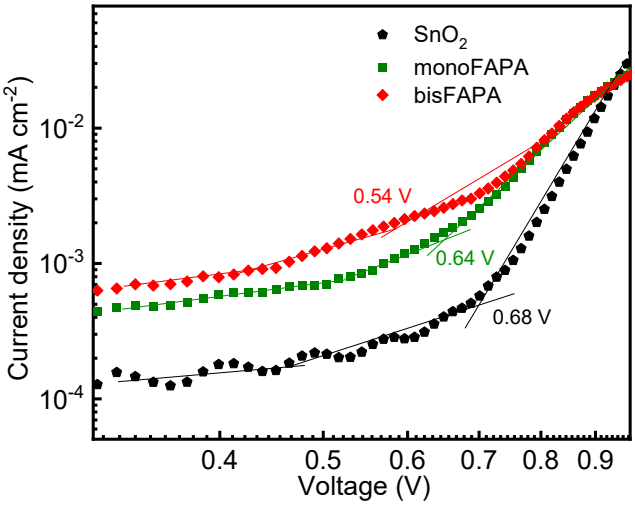

Figure S13. Space-charge-limited current (SCLC) of electron-only devices with SnO_2 interfaces either unmodified or modified with two different FAPA layers.

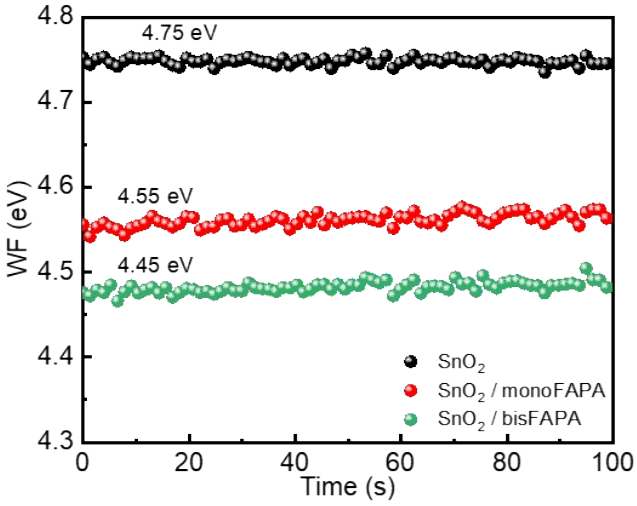

Figure S14. Work function (WF) of SnO_2 and SnO_2 modified with two FAPA measured by Kelvin probe.

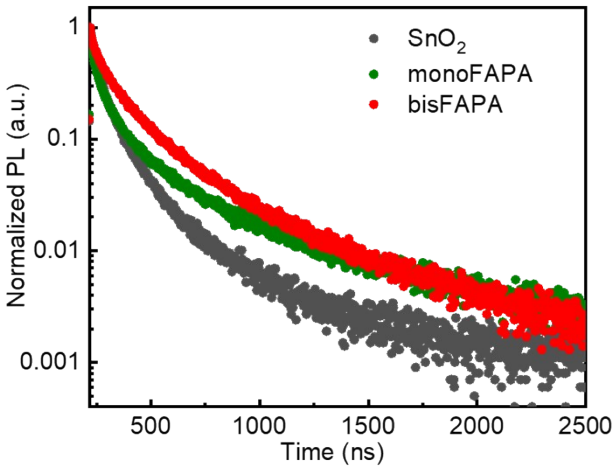

Figure S15. Time-resolved PL lifetime spectra based on SnO_2, monoFAPA and bisFAPA modified SnO_2.

Figure S16. Encapsulated flexible perovskite solar modules.

Figure S17. Damp-heat testing equipment operating at 65°C and 85% relative humidity.

Table S1. Carrier lifetimes extracted from trPL spectra of perovskite on different interfaces.

Layer stack	T_1 (ns)	T_2 (ns)
SnO_2/Perovskite	18	114
SnO_2/monoFAPA/Perovskite	22	195
SnO_2/bisFAPA/Perovskite	36	226

Drift-diffusion simulation (SIMsalabim) and fitting (BOAR)

The drift-diffusion simulations were performed with open-source program SIMsalabim and the fitting with our in-house Bayesian optimization procedure (BOAR). Details about the SIMsalabim and BOAR can be found in their respective GitHub repositories. The fixed parameters for the simulation are detailed in the table below as well as the fitted parameters.

Table S2. Parameters for the drift-diffusion simulation.

Parameter	ITO	SnO_2 | + monoFAPA | + bisFAPA	Perovskite	PEDOT	Carbon	Units
N_c		$2.7 \cdot 10^{24}$	$5 \cdot 10^{24}$	$5 \cdot 10^{26}$		m^{-3}
E_C		4.31 | 4.26 | 4.12	4	5.46		eV
E_V		8.2	5.55	3		eV
L		20	500	30		nm
ε_r		10	24	3		

μ_n $(\times 10^{-5})$		10	0.5		$m^{-2}V^{-1}s^{-1}$
μ_p $(\times 10^{-5})$			3	50	$m^{-2}V^{-1}s^{-1}$
p-doping				$2.5 \cdot 10^{22}$	m^{-3}
C_{ions} $(\times 10^{22})$			3.26		m^{-3}
N_{trap} $(\times 10^{19})$			4 | 4 | 3.8		m^{-3}
$N_{t,int}$		$9.25 \cdot 10^{12}$ | $6.72 \cdot 10^{12}$ | $5.57 \cdot 10^{12}$		$1 \cdot 10^{11}$	m^{-2}
$C_{n,p}$			$1 \cdot 10^{-13}$		m^3s^{-1}
E_{trap}			4.7		eV
k_2			$1 \cdot 10^{-17}$		m^3s^{-1}
$G_{ehp}(\times 10^{}$			2.37 | 2.42 | 2.71		$m^{-3}s^{-1}$
$R_s(\times 10^{-}$			1.80 | 1.12 | 1.02		$\Omega\, m^2$
$R_{sh}(\times 10^{1}$			0.38 |2.14 | 2.14		$\Omega\, m^2$
WF	4.365 | 4.31 |4.31			5.26	eV
ω_{int}		$7.53 \cdot 10^{4}$ | $7.99 \cdot 10^{3}$ | $3.04 \cdot 10^{1}$		$3.18 \cdot 10^{1}$	$m^{-1}s^{-1}$

Parameter Symbol	Name
N_c	Effective density of states
E_C	Conduction band
E_V	Valence band
L	Thickness
ε_r	Relative dielectric constant
$\mu_{n(p)}$	Electron (Hole) mobility
C_{ions}	Ion density
N_{trap}	Bulk trap density
$N_{t,int}$	Interface trap density
$C_{n,p}$	Capture coefficient
E_{trap}	Trap level position
k_2	Radiative recombination rate

G_{ehp}	Average generation rate
R_s	Series resistance
R_{sh}	Shunt resistance
WF	Electrode work function

Interface trap density for simulation

Trap density ($N_{t,int}$) in the bulk of perovskite and at the ETL/perovskite interface are set based on the PL lifetime τ (Table S1) by the following equation[24]:

$$N_{t,int} = \frac{d}{2C} \times \frac{D\pi^2}{D\pi^2\tau_{ETL/pero} - d^2}$$

where d is the thickness of perovskite, C is minority carrier capture coefficient, and D is the diffusion coefficient.

Table S3. Recent advances in f-PSCs with different deposition methods, top electrodes, and upscaling for perovskite solar cells.

Year	Method	Top electrode	Device PCE (%)	Module PCE (%)	Ref.
2017	Spin-coating	Al	17.90	-	1
2018	Spin-coating	Au	16.74	-	2
2019	Spin-coating	Cu	17.03	-	3
2019	Spin-coating	Ag	17.23	-	4
2019	Spin-coating	Ag	18.10	-	5
2019	Spin-coating	Ag	18.53	-	6
2020	Spin-coating	Cu	13.58	-	7
2020	Spin-coating	Carbon	15.18	15.18 (1 cm^2)	8
2020	R2R (SnO_2 and Perovskite)	Au	16.70	-	9
2020	Spin-coating	Ag	17.07	-	10
2020	Spin-coating	Ag	17.30	-	11
2020	Doctor-blading (Perovskite)	Ag	19.41	16.61 (1 cm^2)	12
2020	Doctor-blading	Ag	19.87	17.55 (10 cm^2)	13

2021	Spin-coating	Ag	20.56	-	14
2021	Spin-coating	Au	21.00	-	15
2022	Spin-coating	Au	21.90	-	16
2022	Spin-coating	Ag	23.35	21.52 (1 cm^2)	17
2023	Spin-coating	Ag	23.36	-	18
2023	R2R	Carbon	10.8	-	19
2024	R2R	Carbon/Ag	15.5	11.0%	20
2024	**R2R (SnO_2) Fully printed**	**Carbon**	**17.0**	**11.6%**	**This work**

References:

1. J. H. Heo, D. H. Shin, M. H. Jang, M. L. Lee, M. G. Kang, S. H. Im, J. Mater. Chem. A 2017, 5, 21146.
2. Kim, B. J., Kim, M. C., Lee, D. G., Lee, G., Bang, G. J., Jeon, J. B., ... & Jung, H. S. (2018). Advanced Materials Interfaces, 5(23), 1800993.
3. G. Lee, M.-C. Kim, Y. W. Choi, N. Ahn, J. Jang, J. Yoon, S. M. Kim, J.-G. Lee, D. Kang, H. S. Jung, Energy Environ. Sci. 2019, 12, 3182.
4. S. Cong, G. Zou, Y. Lou, H. Yang, Y. Su, J. Zhao, C. Zhang, P. Ma, Z. Lu, H. Fan, Nano Lett. 2019, 19, 3676.
5. M. Li, Y. G. Yang, Z. K. Wang, T. Kang, Q. Wang, S. H. Turren-Cruz, X. Y. Gao, C. S. Hsu, L. S. Liao, A. Abate, Adv. Mater. 2019, 31, 1901519.
6. N. Zhu, X. Qi, Y. Zhang, G. Liu, C. Wu, D. Wang, X. Guo, W. Luo, X. Li, H. Hu, ACS Appl. Energy Mater. 2019, 2, 3676.
7. P. Li, Z. Wu, H. Hu, Y. Zhang, T. Xiao, X. Lu, Z. Ren, G. Li, Z. Wu, J. Hao, ACS Appl. Mater. Interfaces 2020, 12, 26050.
8. V. Babu, R. Fuentes Pineda, T. Ahmad, A. O. Alvarez, L. A. Castriotta, A. Di Carlo, F. Fabregat-Santiago, K. Wojciechowski, ACS Appl. Energy Mater. 2020, 3, 5126.
9. Kim, Y. Y., Yang, T. Y., Suhonen, R., Kemppainen, A., Hwang, K., Jeon, N. J., & Seo, J. (2020). Nature communications, 11(1), 5146.
10. T. Ahmad, B. Wilk, E. Radicchi, R. Fuentes Pineda, P. Spinelli, J. Herterich, L. A. Castriotta, S. Dasgupta, E. Mosconi, F. De Angelis, Adv. Funct. Mater. 2020, 30, 2004357.
11. M. Li, W. W. Zuo, A. G. Ricciardulli, Y. G. Yang, Y. H. Liu, Q. Wang, K. L. Wang, G. X. Li, M. Saliba, D. Di Girolamo, Adv. Mater. 2020, 32, 2003422.
12. Z. Wang, L. Zeng, C. Zhang, Y. Lu, S. Qiu, C. Wang, C. Liu, L. Pan, S. Wu, J. Hu, Adv. Funct. Mater. 2020, 30, 2001240.
13. X. Meng, Z. Cai, Y. Zhang, X. Hu, Z. Xing, Z. Huang, Z. Huang, Y. Cui, T. Hu, M. Su, Nat. Commun. 2020, 11, 3016.

14. X. Hu, X. Meng, X. Yang, Z. Huang, Z. Xing, P. Li, L. Tan, M. Su, F. Li, Y. Chen, Sci. Bull. 2021, 66, 527.
15. Q. Dong, M. Chen, Y. Liu, F. T. Eickemeyer, W. Zhao, Z. Dai, Y. Yin, C. Jiang, J. Feng, S. Jin, Joule 2021, 5, 1587.
16. Zheng, Z., Li, F., Gong, J., Ma, Y., Gu, J., Liu, X., ... & Liu, M. (2022). Advanced Materials, 34(21), 2109879.
17. Gao, D., Li, B., Li, Z., Wu, X., Zhang, S., Zhao, D., ... & Zhu, Z. (2023). Advanced Materials, 35(3), 2206387.
18. Meng, Y., Liu, C., Cao, R., Zhang, J., Xie, L., Yang, M., ... & Ge, Z. (2023). Advanced Functional Materials, 2214788.
19. Beynon, D., Parvazian, E., Hooper, K., McGettrick, J., Patidar, R., Dunlop, T., ...& Watson, T. (2023). Advanced Materials, 35(16), 2208561.
20. Weerasinghe H C, Macadam N, Kim J E, et al. Nature Communications, 2024, 15(1): 1656.